ORIGINAL RESEARCH
published: 16 June 2020
doi: 10.3389/fmats.2020.00168

Theoretical Design for the Non-Toxic and Earth-Abundant Perovskite Solar Cell Absorber Materials

Chunbao Feng, Guanghui Feng, Qing Zhao, Shichang Li and Dengfeng Li**

School of Science, Chongqing University of Posts and Telecommunications, Chongqing, China

Though perovskite solar cells have good prospects, they also have some disadvantages, especially the impact of Pb on the environment and the use of expensive elements, which makes their production difficult to industrialize. Using first-principle density functional theory, we have investigated the geometric structures, electronic structures, and optical absorption coefficients of non-toxic and earth-abundant 1B-based perovskite solar cell absorbers. Our results show that Cs_2AgAuI_6, a toxin-free and inexpensive AgAu-based perovskite solar cell absorber, is suitable for use. It has a suitable HSE bandgap (1.289 eV) and a sharp absorption coefficient ($\sim 10^5$ cm^{-1}). Meanwhile, it is beneficial to the average electron and hole effective masses are 0.346 and 0.316 m_0 respectively. The phonon spectra show that it is stable. Because the *d*-orbital energy of Cu is higher than those of Ag and Au, CuAu-based perovskite is not stable. This can be seen from the phonon spectra. Therefore, our calculations could provide strong evidence for the experimental synthesis of lead-free and low-cost perovskite solar cell absorber materials.

Keywords: perovskite solar cell, lead-free, earth-abundant, first-principles calculation, high absorption coefficient

OPEN ACCESS

Edited by:
Zhenyu Li,
University of Science and Technology of China, China

Reviewed by:
Youyong Li,
Soochow University, China
Yafei Li,
Nanjing Normal University, China

***Correspondence:**
Chunbao Feng
fengcb@cqupt.edu.cn
Dengfeng Li
lidf@cqupt.edu.cn

Specialty section:
This article was submitted to Computational Materials Science, a section of the journal Frontiers in Materials

Received: *26 February 2020*
Accepted: *06 May 2020*
Published: *16 June 2020*

Citation:
Feng C, Feng G, Zhao Q, Li S and Li D (2020) Theoretical Design for the Non-Toxic and Earth-Abundant Perovskite Solar Cell Absorber Materials. Front. Mater. 7:168. doi: 10.3389/fmats.2020.00168

INTRODUCTION

In the space of <10 years, Perovskite solar cell (PSCs) material has gradually become a star material in the field of solar photovoltaic conversion. It has excellent photoelectric conversion efficiency (PCE), which has grown from 3.8 to 25.2% (Kojima et al., 2009; NREL Efficiency Chart Vol, 2019). The structural formula of a perovskite solar cell is $AM^{IV}X^{VII}{}_3$. Nowadays, A can be not only a small organic molecule [$A^1 = CH_3NH_3^+$, $CH(NH_2)_2^+$] but also a low-valent group-IA metal cation ($A^2 = Cs^+$, Na^+, and Rb^+), M^{IV} represents a divalent group-IVA metal cation ($M^{IV} = Pb^{2+}$, Sn^{2+}), and X is a halogen (X = Cl, Br, and I). This tremendous progress is because of its superior optoelectronic properties: suitable band gaps, a high tolerance factor (Gao et al., 2019), long carrier diffusion length (Stranks et al., 2013), low exciton binding energy (Lee et al., 2012; Burschka et al., 2013), and balanced electron and hole mobility (Stoumpos et al., 2013; Ponseca et al., 2014). These advantages make us more confident in researching and exploring perovskite solar cell materials.

Although the current perovskite solar cells have seen great success in theoretical research, there are still some great challenges in their practical application and large-scale commercial production. The first urgent problem to be solved is the stability of devices using perovskite material, especially devices that are under high temperature or a humid environment. This may be due to the loose chemical bonds between the organic cations and their inherent instability (Kulbak et al., 2015; Niu et al., 2015; Sutton et al., 2016). Recently, studies have shown that partial replacement of MA by FA can significantly improve the thermal stability of hybrid perovskite (Hu et al., 2014; Pellet et al., 2014; Binek et al., 2015). Therefore, in this paper, we will use the element Cs to replace the organic cation and research the various properties of the resulting perovskite solar cell materials. The second is the use of Pb in the perovskite materials, because it is a toxic element and is very harmful to our living environment. Therefore, we need to replace it but without affecting the photovoltaic conversion efficiency. Many researchers have used Sn to replace Pb, but Sn^{2+} is easily oxidized in air to Sn^{4+}, and compared with lead-containing perovskite solar cells, devices with Sn-based perovskite materials have lower PCEs, e.g., that of $MASnI_3$ is only about 6% and that of $CsSnI_3$ is only about 3.5% (Hao et al., 2014; Noel et al., 2014). Therefore, researchers have considered converting two Pb^{2+} into IB group (Ag^+, Au^+, and Cu^+) and IIIA group (In^{3+}, Bi^{3+}, and Ga^{3+}) elements to keep the same valence number at M^{IV} sites (Du et al., 2017; Meng et al., 2017; Slavney et al., 2017; Volonakis et al., 2017; Wei et al., 2017; Zhao et al., 2017) and design lead-free halide double-perovskite $A_2M^+M^{3+}X_6^{VII}$. This work provides us with an idea to guide our exploration of inorganic non-toxic halide double-perovskite solar cells.

Recently, research has focused on the non-toxic inorganic mixed-valence double-perovskite solar cell absorption layer material $Cs_2Au_2I_6$ (Matsushita et al., 2005; Castro-Castro and Guloy, 2010; Debbichi et al., 2018; Giorgi et al., 2018), where the Au element has a mixed valency of +1 and +3 (Liu et al., 1999). This material has a direct bandgap (~1.3 eV) and good stability and photoelectric conversion efficiency. However, a disadvantage is that Au is an expensive metal element, so this material is difficult to commercialize and industrialize.

In this paper, our results show that Cs_2AgAuI_6, a non-toxic and inexpensive AgAu-based perovskite solar cell absorber, is a suitable alternative. It has a suitable HSE bandgap (1.289 eV) and a sharp absorption coefficient ($\sim 10^5$ cm^{-1}). Meanwhile, it is beneficial to the average effective masses of electron and hole carriers, 0.346 and 0.316 m_0, respectively. This is almost the same as that of $MAPbI_3$. The phonon spectra show that it is stable. Because the *d*-orbital energy of Cu is higher than those of Ag and Au, CuAu-based perovskite is not stable. This can be seen from the phonon spectra. Therefore, our calculations could provide strong evidence for the experimental synthesis of lead-free and low-cost perovskite solar cell absorber materials.

COMPUTATIONAL METHODS

Our first-principles calculations were performed on the basis of density-functional theory (DFT) methods by using the Vienna *Ab Initio* Simulation Package (VASP) code (Kresse and Furthmüller, 1996) and the standard frozen-core projector augmented-wave (PAW) methods (Kresse and Joubert, 1999). In the calculation, we used the generalized gradient approximation of Perdew, Burke, and Ernzerhof (PBE) (Perdew et al., 1996) as the exchange-correlation functional to optimize the structures and calculate band gaps. In order to reduce the self-interaction error of DFT in bandgap calculation, we used the Heyd-Scuseria-Ernzerhof (HSE) of the standard hybrid density functional with 25% exact Fock exchange (Krukau et al., 2006). The cutoff energy for the plane wave function was 400 eV. The structures are relaxed until total energies are converged to 10^{-8} eV, and the k-point meshes have a grid spacing of $2\pi \times 0.02$ Å^{-1}. The force on all atoms was $<3 \times 10^{-3}$ eV·Å^{-1}. The $6 \times 6 \times 6$ k-grid was used for density of states (DOS) and optical absorption coefficient calculation of halide perovskite. For the calculation of the phonon spectrum, the finite difference method was implemented in Phonopy code (Togo and Tanaka, 2015), and we constructed a $2 \times 2 \times 2$ supercell of perovskite structures. The force constant was obtained by considering phonon-phonon interaction with the calculation of VASP. The phonon spectrum was acquired by processing the data in Phonopy. MD simulations of a $3 \times 3 \times 3$ supercell with 270 atoms were implemented at room temperature (300 K) with VASP code using the canonical ensemble with a Nose–Hoover thermostat (Hoover, 1985) under an energy cutoff of 300 eV with 1,000 steps under a time step of 1.0 fs. The properties of the electronic structure and optics were obtained using the VASPKIT program (Wang et al., 2019).

RESULTS AND DISCUSSION

Firstly, we established the most stable crystal structure. Here, we choose ABX_3 of four different crystal structures belonging to the space groups P*m-3m*, I4/*mmm*, P*63*/*mmc*, and P*nma*, respectively. The different total energies referring to the most stable configuration (I4/*mmm*) are 0.376, 0, 0.671, and 0.110 eV. In our DFT calculation, we thus use the structure with the I4/*mmm* space group, shown in **Figure 1a**. The most stable one, with the cell parameter 8.647 Å, is consistent with the previous experimental result (Debbichi et al., 2018).

Then, we established a suitable double perovskite crystal structure. We see that $Cs_2M^+M^{3+}X_6^{VII}$ has four different crystal structures because there are four different cation sites in Au-based perovskite. In our calculation, the most stable ones can be seen in **Figures 1b,c**. Both of them have the same perovskite structure symmetry and it should be easier to form for junctions with low non-radiative recombination.

The Goldschmidt tolerance factor (t) can be used as an empirical index to evaluate the structural stability of the perovskite (Kieslich et al., 2015; Shi et al., 2016; Travis et al., 2016), and for $AM^{IV}X^{VII}{}_3$ perovskite, t is defined as:

$$\boldsymbol{t = \frac{R_A + R_X}{\sqrt{2}\,(R_M + R_X)}}$$

where R_A, R_M, and R_X represent the effective ion radii of the A, M site cation and X site anion, respectively. For double perovskite $A_2M^+M^{3+}X_6^{VII}$, the Goldschmidt tolerance factor t for the M site $R_M = \frac{R_M^+ + R_M^{3+}}{2}$. Generally speaking, the lower the symmetry index of the structure, the lower the Goldschmidt tolerance factor t. When $t = 1$, it is an ideal cubic perovskite structure; the range $0.9 \leq t \leq 1$ is generally considered to be very suitable of perovskite, indicating the possibility of a cubic structure; in the range of $0.71 \leq t \leq 0.9$, it indicates that

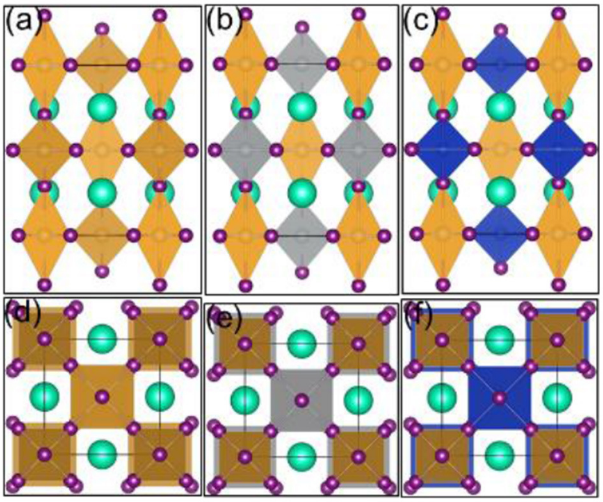

FIGURE 1 | 1B-based perovskite solar cell absorber crystal structures: **(a)** $Cs_2Au(I)Au(III)I_6$, **(b)** $Cs_2Ag(I)Au(III)I_6$, **(c)** $Cs_2Cu(I)Au(III)I_6$: side view; **(d)** $Cs_2Au(I)Au(III)I_6$, **(e)** $Cs_2Ag(I)Au(III)I_6$, **(f)** $Cs_2Cu(I)Au(III)I_6$: top view. Yellow, gray, and blue shapes represent Au, Ag, and Cu atoms, respectively. Visualization was performed with VESTA (Momma and Izumi, 2008).

due to the inclination of the MX_6 octahedron, a rhombohedral or orthorhombic structure may be formed; when $t < 0.71$, it will change the unstable perovskite structure. In our results, the tolerance factor is 0.827, 0.906, and 0.932 for $Cs_2Au_2I_6$, Cs_2AgAuI_6, and Cs_2CuAuI_6, respectively. This means that it is possible to form the cubic perovskite structure for all of them. This is consistent with our calculation, as shown in **Figure 1**. In addition, we performed *ab initio* molecular dynamics (AIMD) simulations to evaluate the thermal stability of Cs_2AgAuI_6. As shown in **Figure S1**, the structures during 1.0ps AIMD simulation maintain the perovskite structure, indicating that Cs_2AgAuI_6 is thermally stable.

As we know, the thermodynamic stability of photovoltaic materials should be stable under all possible decomposition pathways. The decomposition pathways of $Cs_2Au_2I_6$, Cs_2AgAuI_6, and Cs_2CuAuI_6 can be seen in **Table S1**. The enthalpy of decomposition (ΔH_d) is the amount of energy that a substance gains during a reaction, which is the difference between the sum of the energies of each substance that is obtained after the reaction and the energies of the reactants themselves. A positive ΔH means that the reaction is endothermic; it means that the reactant itself is very stable and needs to absorb energy from the outside to react, which results in suppressed decomposition of $Cs_2Au_2I_6$, Cs_2AgAuI_6, and Cs_2CuAuI_6 and shows that the structure is stable.

As can be seen in **Table S1**, we would be able to synthesize $Cs_2Au_2I_6$ much more easily than $MAPbI_3$ because the dissociation energy of the former is larger than that of the latter (Yin et al., 2014a; Debbichi et al., 2018). We also find that we should avoid forming the secondary phase AuI_3 by carefully controlling the growth conditions. Although some of the decomposition enthalpies of Cs_2CuAuI_6 are larger than that of Cs_2AgAuI_6, it would be difficult to form the former if we found the secondary phases (for example CuI_2, $CsCuI_3$) in the experiment. Meanwhile, we should also be much more careful to control the experimental conditions to form Cs_2CuAuI_6 and Cs_2AgAuI_6 so as to avoid any of the secondary phases (for example, CuI, AgI, $CsCu_2I_3$, $CsAg_2I_3$, $CsCuI_3$, and $CsAuI_3$) forming. Also, it is more important to avoid the secondary phase $Cs_2Au_2I_6$ forming in the experiment if we would want to synthesize Cs_2CuAuI_6 and Cs_2AgAuI_6.

In solar cell devices, the photo-generated carriers can be effectively collected along the electrodes. The effective mass of carriers is one of the important factors that determine the carrier mobility. Therefore, we choose the ideal semiconductor materials, which should have light effective masses of the electron (m_e^*) and hole (m_h^*). The effective mass of the photo-generated carrier can be approximately fitted around the band edge by:

$$m^* = \hbar^2 \left[\frac{\partial^2 \varepsilon\left(k\right)}{\partial k^2} \right]^{-1},$$

where k represents the wave vector along different directions and $\varepsilon\left(k\right)$ represents the eigenvalue of energy on the band.

From our results, the effective masses of the electron (m_e^*) and hole (m_h^*) are clearly comparable among various semiconductor materials. $Cs_2Au_2I_6$ is more suitable as a perovskite solar cell material, as it has heavy effective masses of the electron (m_e^*) and hole (m_h^*) at point N in **Figure 2** of $0.362m_0$ and $0.371m_0$. In previous research, $MAPbI_3$ perovskite solar cells have been shown to have good electronic and optical properties. It was found that the effective mass of its electron (m_e^*) is 0.32 m_0 and of the hole (m_h^*) is 0.36 m_0 (Giorgi et al., 2013; Yin et al., 2014b). This further indicates that when perovskite solar cells have lower effective masses of electrons and holes, their photo-generated carriers will be better collected by the electrodes and have higher photoelectric conversion efficiency. For Cs_2AgAuI_6, the heavy effective masses of the electron (m_e^*) and hole (m_h^*) are 0.548 and 0.494 m_0, while for Cs_2CuAuI_6, the effective masses of the electron (m_e^*) and hole (m_h^*) are heavier, 0.754 and 0.572 m_0. It is clear that the effective masses of the electron and hole in Cs_2AgAuI_6 and Cs_2CuAuI_6 are much larger than those in $CsAuI_3$. This is because the d orbital of Ag and Cu is higher than that of Au, so the VBM is much more localized in Cs_2AgAuI_6 and Cs_2CuAuI_6 than in $Cs_2Au_2I_6$, and the VBM is much more dispersive in $Cs_2Au_2I_6$ than in Cs_2AgAuI_6 and Cs_2CuAuI_6. This can be seen in **Figure 2**.

Although PBE or HSE+SOC calculations sometimes give a bandgap result that approaches experimental values (Yin et al., 2014a; Du, 2015), the most recent calculation shows that the HSE calculation of the $Cs_2Au_2I_6$ system approaches the experiment results. As shown in **Figure S2**, the relative band gap between PBE and PBE+SOC calculations is only around 0.1 eV. From **Figure 2**, the bandgap of $Cs_2Au_2I_6$ obtained with HSE calculation is 1.167 eV; this is consistent with recent theoretical reports (∼1.3 eV) (Giorgi et al., 2018) and is close to a previous experimental result, which gave a value of 1.31 eV (Debbichi et al., 2018). This indicates that $Cs_2Au_2I_6$ lacks strong exciton binding energy, so it is easier to produce a free election and

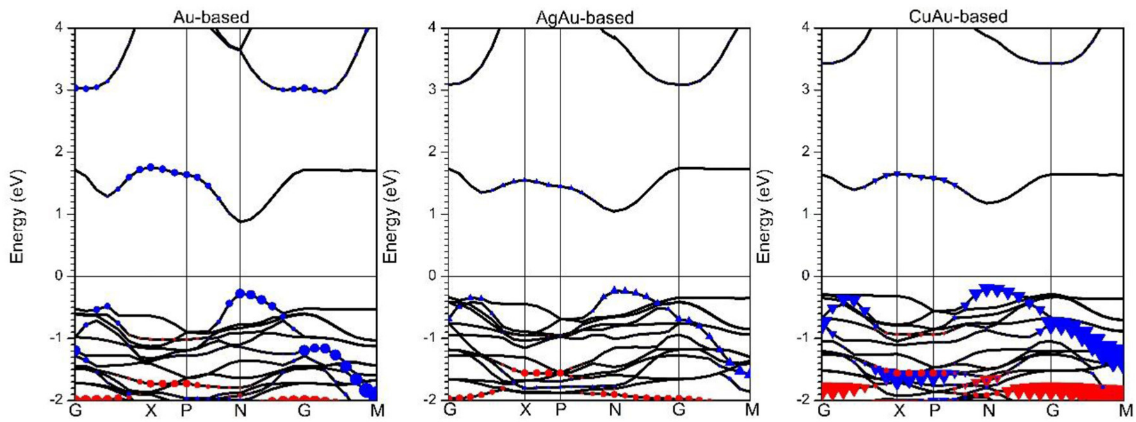

FIGURE 2 | The HSE band structures of 1B-based perovskite solar cell absorbers. Blue and red shapes indicate the dz^2 and dx^2-y^2 orbitals of 1B atoms, respectively. Circles, triangles, and inverted triangles represent Au, Ag, and Cu atoms contributions, respectively.

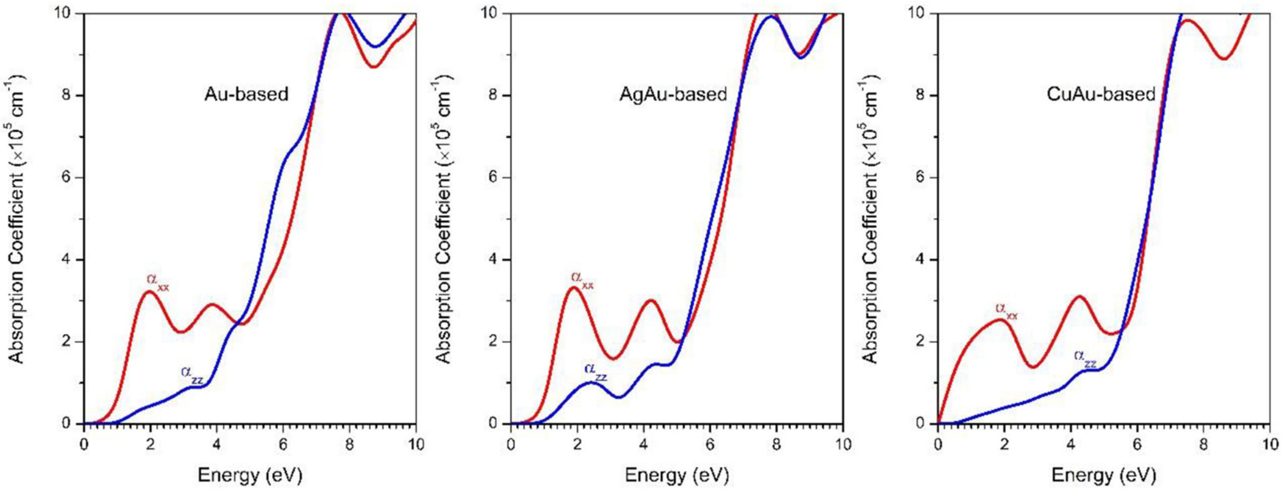

FIGURE 3 | The HSE optical absorption coefficients of 1B-based perovskite solar cell absorbers.

hole after photoexcitation; at the same time, the G→M band gap is relatively flat, which indicates that $Cs_2Au_2I_6$ has two-dimensional or one-dimensional properties (Saparov et al., 2016; Xiao et al., 2016). At the same time, **Figure 2** shows that the HSE band gaps of Cs_2AgAuI_6 and Cs_2CuAuI_6 are 1.289 and 1.344 eV, respectively. It is clearly seen that the band edge of $Cs_2Au_2I_6$ is the d-orbital of the Au atom, while the band edge of Cs_2AgAuI_6 and Cs_2CuAuI_6 is the d-orbital of the Ag and Cu atoms, respectively. This is because the *d* electron energy of Ag and Cu atoms is higher than the *d* electron energy of an Au atom (Kojima and Kitagawa, 1994). This was also confirmed by the PDOS in **Figure S3**. In **Figure 2**, it can be seen at band edges along the G→M direction have flat conduction and valance bands, and the possibility of carrier mobility has huge anisotropy along out-of-plane and in-plane direction; this is due to $Cs_2Au_2I_6$ having different 5*d*-orbital splitting of elongated $Au^{3+}(d^8)I_6$ octahedra and compressed $Au^{+}(d^{10})I_6$ octahedra (Liu et al., 1999; Tang et al., 2019), and Cs_2AgAuI_6 at the band edge also has two different *d* metal cations, indicating that $Cs_2Au_2I_6$ and Cs_2AgAuI_6 have 2D electronic properties in 3D materials (Tang et al., 2019). Meanwhile, the bandgap edges of the N→P direction shows an obvious dispersion band edge. We calculated that $Cs_2Au_2I_6$ has light effective masses of the electron (m_e^*) and hole (m_h^*) of 0.145 and 0.137 m_0 and that those of Cs_2AgAuI_6 are 0.310 and 0.218 m_0, indicating that the carriers are easier to move. This is due to the Au and I orbitals forming an anti-bonding overlap so that there is larger dispersion. We found that the band gap of $Cs_2Au_2I_6$ is almost the same as that of Cs_2AgAuI_6 is the ideal material that we were looking for.

It should be noted that the optimal solar cell absorbers should have a direct bandgap and high optical absorption with *p-p* optical transition (Yin et al., 2014b). Although 1B-based perovskites have *d-d* optical transition, they also have comparatively high optical absorption ($\sim 10^5$ cm^{-1}) (**Figure 3**). This is consistent with previous research on semiconductors with *d-d* transitions (Heo et al., 2017). From our results, we found that

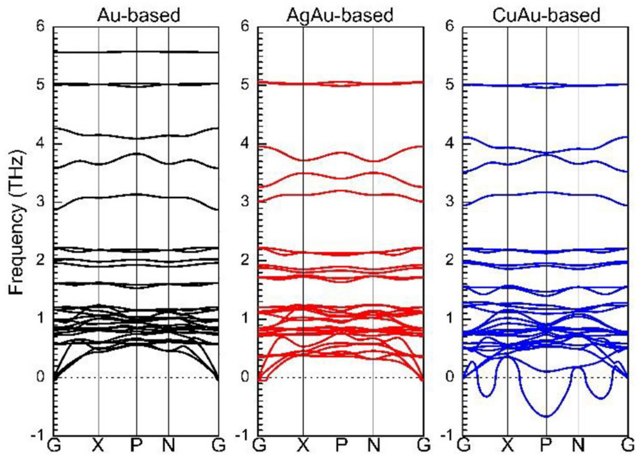

FIGURE 4 | Calculated phonon spectra of $Cs_2Au_2I_6$, Cs_2AgAuI_6, and Cs_2CuAuI_6, respectively.

TABLE 1 | The structural parameters (Å), PBE band gap (eV), and HSE band gap (eV) of 1B-based perovskite solar cell absorbers.

1B-based PVSK		PBE lattice parameters (Å)	PBE band gap (eV)	HSE band gap (eV)
Au-based PVSK	Cl	7.808	0.931	1.591
	Br	8.139	0.748	1.264
	I	8.647	0.770	1.167
AgAu-based PVSK	Cl	7.804	0.812	1.566
	Br	8.152	0.740	1.369
	I	8.687	0.763	1.289
CuAu-based PVSK	Cl	7.657	0.647	1.982
	Br	8.021	0.688	1.487
	I	8.561	0.838	1.344

the optical absorption of the 1B-based perovskites has strongly anisotropic properties. There is different optical absorption for the directions parallel and perpendicular to the z-axis. This is in good agreement with previous experimental and theoretical results (Debbichi et al., 2018; Giorgi et al., 2018). Our results show that the optical absorptions of $Cs_2Au_2I_6$ and Cs_2AgAuI_6 are very similar. This is because both of them have a similar band structure. Meanwhile, we found that the optical absorption along the zz direction of Cs_2AgAuI_6 is stronger than that of $Cs_2Au_2I_6$. This is because the bond length between the cation and I became longer when we use Ag atom substitution of an Au atom in $Cs_2Au_2I_6$. As can be seen from **Table 1**, the lattice constant of Cs_2AgAuI_6 is a little larger than that of $Cs_2Au_2I_6$. Then, the *d-d* transition became weaker in Cs_2AgAuI_6, so the optical absorption coefficient will become stronger in Cs_2AgAuI_6.

Through **Figure 4**, we can clearly see that $Cs_2Au_2I_6$ and Cs_2AgAuI_6 are stable, even if the system of $Cs_2Au_2I_6$ and Cs_2AgAuI_6 has a lower virtual frequency; this may be due to the strong Coulomb interaction between metal elements, and the virtual frequency is within reasonable limits. In this study, we tried to dope with other elements the reduce the amount of Au needed. The phonon spectra calculation from our research indicates that Cs_2AgAuI_6 is very stable, contrary to Cs_2CuAuI_6, and so a Cu-based perovskite solar cell absorber would be difficult to synthesize. This is clearly shown in **Figure 2** the d band energy of the Cu atom is higher than that of the Ag and Au atoms. This result is consistent with the previous calculation (Xiao et al., 2017).

The calculated bandgaps and the geometric parameters are summarized in **Table 1**. The picture painted by our results could provide practical guidance for choosing the appropriate compositions to harvest good solar-to-solar cell absorbers. For example, for a two-junction tandem solar cell configuration that obtains the best conversion efficiency, the top and bottom cell should be made of semiconductors with bandgaps of 1.9 and 1.0 eV. **Table 1** suggests that $Cs_2CuAuCl_6$ could be chosen for the top cell and $Cs_2Au_2I_6$ could be chosen for the bottom cell. For a three-junction configuration, the semiconductors for the top, middle, and bottom cells should have bandgaps of 2.3, 1.4, and 0.8 eV, respectively. Accordingly, **Table 1** suggests $Cs_2Au_2(Br_{1-x}Cl_x)_6$ and $Cs_2AgAu(Br_{1-x}Cl_x)_6$ for the middle cell and $Cs_2Au_2I_6$ for the bottom cell, though there is no optimal composition for the top cell. Our results show that all of the compositions in **Table 1** with the same perovskite structure should be easier to form for junctions with low non-radiative recombination.

CONCLUSIONS

In the paper, we researched the crystal structures, electronic structures, and optical properties of 1B-based perovskite solar cell absorbers by using the density-functional theory. Our results show that Cs_2AgAuI_6, a non-toxic and inexpensive AgAu-based perovskite solar cell absorber, may be a good choice. It has a suitable HSE band gap (1.289 eV) and a sharp absorption coefficient ($\sim10^5$ cm^{-1}). Meanwhile, it is beneficial to the average effective masses of the electron and hole carrier, 0.346 and 0.316 m_0, respectively. The phonon spectra show that it is stable. Because the *d*-orbital energy of Cu is higher than those of Ag and Au, CuAu-based perovskite is not stable. This can be seen from the phonon spectra. Therefore, our calculations could provide strong evidence for experimental synthesis of lead-free and low-cost perovskite solar cell absorber materials.

DATA AVAILABILITY STATEMENT

The raw data supporting the conclusions of this article will be made available by the authors, without undue reservation, to any qualified researcher.

AUTHOR CONTRIBUTIONS

CF conceived the idea and performed the calculations. All authors analyzed the results and wrote the paper.

FUNDING

This work was supported by funding from the National Natural Science Foundation of China (under Grant No. 11604035).

SUPPLEMENTARY MATERIAL

The Supplementary Material for this article can be found online at: https://www.frontiersin.org/articles/10.3389/fmats.2020.00168/full#supplementary-material

REFERENCES

Binek, A., Hanusch, F. C., Docampo, P., and Bein, T. (2015). Stabilization of the trigonal high-temperature phase of formamidinium lead iodide. *J. Phys. Chem. Lett.* 6, 1249–1253. doi: 10.1021/acs.jpclett.5b00380

Burschka, J., Pellet, N., Moon, S.-J., Humphry-Baker, R., Gao, P., Nazeeruddin, M. K., et al. (2013). Sequential deposition as a route to high-performance perovskite-sensitized solar cells. *Nature* 499, 316–319. doi: 10.1038/nature12340

Castro-Castro, L. M., and Guloy, A. M. (2010). Organic-based layered perovskites of mixed-valent gold(I)/gold(III) iodides. *Angew. Chem. Int. Ed.* 115, 2877–2880. doi: 10.1002/ange.200350929

Debbichi, L., Lee, S., Cho, H., Rappe, A. M., Hong, K.-H., Jang, M. S., et al. (2018). Mixed valence perovskite $Cs_2Au_2I_6$: a potential material for thin-film pb-free photovoltaic cells with ultrahigh efficiency. *Adv. Mater.* 30:1707001. doi: 10.1002/adma.201707001

Du, K.-Z., Wang, X. M., Han, Q. W., Yan, Y. F., and Mitzi, D. B. (2017). Heterovalent B-site Co-alloying approach for halide perovskite bandgap engineering. *ACS Energy Lett.* 2, 2486–2490. doi: 10.1021/acsenergylett.7b00824

Du, M.-H. (2015). Density functional calculations of native defects in $CH_3NH_3PbI_3$: effects of spin–orbit coupling and self-interaction error. *J. Phys. Chem. Lett.* 68, 1461–1466. doi: 10.1021/acs.jpclett.5b00199

Gao, F., Zhao, Y., Zhang, X., and You, J. (2019). Recent progresses on defect passivation toward efficient perovskite solar cells. *Adv. Energy Mater.* 10:1902650. doi: 10.1002/aenm.201902650

Giorgi, G., Fujisawa, J.-I., Fujisawa, H., and Yamashita, K. J. (2013). Small photocarrier effective masses featuring ambipolar transport in methylammonium lead iodide perovskite: a density functional analysis. *Phys. Chem. Lett.* 4, 4213–4216. doi: 10.1021/jz4023865

Giorgi, G., Yamashita, K., and Palummo, M. (2018). Two-dimensional optical excitations in the mixed-valence $Cs_2Au_2I_6$ fully inorganic double perovskite. *J. Mater. Chem. C.* 6, 10197–10201. doi: 10.1039/C8TC03496F

Hao, F., Stoumpos, C. C., Cao, D. H., Chang, R. P. H., and Kanatzidis, M. G. (2014). Lead-free solid-state organic–inorganic halide perovskite solar cells. *Nat. Photonics* 8, 489–494. doi: 10.1038/nphoton.2014.82

Heo, J., Yu, L., Altschul, E., Waters, B. E., Wager, J. F., Zunger, A., et al. (2017). $CuTaS_3$: intermetal *d-d* Transitions Enable High Solar Absorption. *Chem. Mater.* 29, 2594–2598. doi: 10.1021/acs.chemmater.6b04730

Hoover, W. G. (1985). Canonical dynamics: equilibrium phase-space distributions. *Phys. Rev. A* 31:1695. doi: 10.1103/PhysRevA.31.1695

Hu, M., Liu, L., Mei, A., Yang, Y., Liu, T., and Han, H. (2014). Efficient hole-conductor-free, fully printable mesoscopic perovskite solar cells with a broad light harvester $NH_2CH{=}NH_2PbI_3$. *J. Mater. Chem. A* 2, 17115–17121. doi: 10.1039/C4TA03741C

Kieslich, G., Sun, S., and Cheetham, A. (2015). An extended Tolerance Factor approach for organic–inorganic perovskites. *Chem. Sci.* 6, 3430–3433. doi: 10.1039/C5SC00961H

Kojima, A., Teshima, K., Teshima, Y., and Miyasaka, T. (2009). Organometal halide perovskites as visible-light sensitizers for photovoltaic cells. *J. Am. Chem. Soc.* 131, 6050–6051. doi: 10.1021/ja809598r.

Kojima, N., and Kitagawa, H. (1994). Optical investigation of the intervalence charge-transfer interactions in the three-dimensional gold mixed-valence compounds Cs_2AuX_6 (X = Cl, Br or I). *J. Chem. Soc. Dalton Trans.* 3, 327–331. doi: 10.1039/dt9940000327

Kresse, G., and Furthmüller, J. (1996). Efficiency of ab-initio total energy calculations for metals and semiconductors using a plane-wave basis set. *Comput. Mater. Sci.* 6, 15–50. doi: 10.1016/0927-0256(96)00008-0

Kresse, G., and Joubert, D. (1999). From ultrasoft pseudopotentials to the projector augmented-wave method. *Phys. Rev. B.* 59:1758. doi: 10.1103/PhysRevB.59.1758

Krukau, A. V., Vydrov, O. A., Izmaylov, A. F., and Scuseria, G. E. (2006). Influence of the exchange screening parameter on the performance of screened hybrid functionals. *J. Chem. Phys.* 125:224106. doi: 10.1063/1.2404663

Kulbak, M., Cahen, D., and Hodes, G. (2015). How important is the organic part of lead halide perovskite photovoltaic cells? efficient $cspbbr_3$ cells. *J. Phys. Chem. Lett.* 6, 2452–2456. doi: 10.1021/acs.jpclett.5b00968

Lee, M. M., Teuscher, J., Miyasaka, T., Murakami, T. N., and Snaith, H. J. (2012). Efficient hybrid solar cells based on meso-superstructured organometal halide perovskites. *Science* 338, 643–647. doi: 10.1126/science.1228604

Liu, X. J., Matsuda, K., Moritomo, Y., Nakamura, A., and Kojima, N. (1999). Electronic structure of the gold complexes $Cs_2Au_2X_6$ (X=I, Br, and Cl). *Phys. Rev. B.* 59, 7925. doi: 10.1103/PhysRevB.59.7925

Matsushita, N., Fukuhara, F., and Kojima, N. (2005). A three-dimensional bromo-bridged mixed-valence gold(I,III) compound, $Cs_2Au(I)Au(III)Br_6$. *Acta. Crystallogr. E.* 61, i123–i125. doi: 10.1107/S1600536805016594

Meng, W. W., Wang, X. M., Xiao, Z. W., Wang, J. B., Mitzi, D. B., and Yan, Y. F. (2017). Parity-forbidden transitions and their impact on the optical absorption properties of lead-free metal halide perovskites and double perovskites. *J. Phys. Chem. Lett.* 8, 2999–3007. doi: 10.1021/acs.jpclett.7b01042

Momma, K., and Izumi, F. (2008). VESTA: a three-dimensional visualization system for electronic and structural analysis. *J. Appl. Crystallogr.* 41, 653–658. doi: 10.1107/S0021889808012016

Niu, G., Guo, X., and Wang, L. (2015). Review of recent progress in chemical stability of perovskite solar cells. *J. Mater. Chem. A* 3, 8970–8980. doi: 10.1039/C4TA04994B

Noel, N. K., Stranks, S. D., Abate, A., Wehrenfennig, C., Guarnera, S., Haghighirad, A.-A., et al. (2014). Lead-free organic–inorganic tin halide perovskites for photovoltaic applications. *Energy Environ. Sci.* 7, 3061–3068. doi: 10.1039/C4EE01076K

NREL, Efficiency Chart Vol (2019) https://www.nrel.gov/pv/cell-efficiency.html

Pellet, N., Gao, P., Gregori, G., Yang, T.-Y., Nazeeruddin, M. K., Maier, J., et al. (2014). Mixed-organic-cation perovskite photovoltaics for enhanced solar-light harvesting. *Angew. Chem. Int. Ed.* 126, 3215–3221. doi: 10.1002/ange.201309361

Perdew, J. P., Burke, K., and Ernzerhof, M. (1996). Generalized gradient approximation made simple. *Phys. Rev. Lett.* 77, 3865–3868. doi: 10.1103/PhysRevLett.77.3865

Ponseca, C. S. Jr., Savenije, T. J., Abdellah, M., Zheng, K., Yartsev, A., Pascher, T., et al. (2014). Organometal halide perovskite solar cell materials rationalized: ultrafast charge generation, high and microsecond-long balanced mobilities, and slow recombination. *J. Am. Chem. Soc.* 136, 5189–5192. doi: 10.1021/ja412583t

Saparov, B., Sun, J.-P., Meng, W. W., Xiao, Z. W., Duan, H.-S., Gunawan, O., et al. (2016). Thin-film deposition and characterization of a Sn-deficient perovskite derivative Cs_2SnI_6. *Chem. Mater.* 28, 2315–2322. doi: 10.1021/acs.chemmater.6b00433

Shi, C., Yu, C.-H., and Zhang, W. (2016). Predicting and screening dielectric transitions in a series of hybrid organic–inorganic double perovskites via an extended tolerance factor approach. *Angew. Chem, Int. Ed.* 128, 5892–5896. doi: 10.1002/ange.201602028

Slavney, A. H., Leppert, L., Bartesaghi, D., Gold-Parker, A., Toney, M. F., Savenije, T. J., et al. (2017). Defect-induced band-edge reconstruction of a bismuth-halide double perovskite for visible-light absorption. *J. Am. Chem. Soc.* 139, 5015–5018. doi: 10.1021/jacs.7b01629

Stoumpos, C. C., Malliakas, C. D., and Kanatzidis, M. G. (2013). Semiconducting tin and lead iodide perovskites with organic cations: phase transitions, high mobilities, and near-infrared photoluminescent properties. *Inorg. Chem.* 52, 9019–9038. doi: 10.1021/ic401215x

Stranks, S. D., Eperon, G. E., Grancini, G., Menelaou, C., Alcocer, M. J. P., Leijtens, T., et al. (2013). Electron-hole diffusion lengths exceeding 1 micrometer in an organometal trihalide perovskite absorber. *Science* 342, 341–344. doi: 10.1126/science.1243982

Sutton, R. J., Eperon, G. E., Miranda, L., Parrott, E. S., Kamino, B. A., Patel, J. B., et al. (2016). Bandgap-tunable cesium lead halide perovskites with high thermal stability for efficient solar cells. *Adv. Energy Mater.* 6, 1502458. doi: 10.1002/aenm.201502458

Tang, G., Xiao, Z., and Hong, J. (2019). Designing two dimensional properties in there dimensional halide perovskite via orbital engineering. *J. Phys. Chem. Lett.* 10, 6688–6694. doi: 10.1021/acs.jpclett.9b02530

Togo, A., and Tanaka, I. (2015). First principles phonon calculations in materials science. *Scr. Mater.* 108, 1–5. doi: 10.1016/j.scriptamat.2015.07.021

Travis, W., Glover, E. N. K., Bronstein, H., Scanlon, D. O., and Palgrave, R. G. (2016). On the application of the tolerance factor to inorganic and hybrid halide perovskites: a revised system. *Chem. Sci.* 7, 4548–4556. doi: 10.1039/c5sc04845a

Volonakis, G., Haghighirad, A. A., Milot, R. L., Sio, W. H., Filip, M. R., Wenger, B., et al. (2017). $Cs_2InAgCl_6$: a new lead-free halide double perovskite with direct band gap. *J. Phys. Chem. Lett.* 8, 772–778. doi: 10.1021/acs.jpclett.6b02682

Wang, V., Xu, N., Liu, J.-C., Tang, G., and Geng, W. (2019). VASPKIT: a pre- and post- processing program for VASP code. *arXiv preprint arXiv:*1908.08269.

Wei, F. X., Deng, Z. Y., Sun, S. J., Zhang, F. H., Evans, D. M., Kieslich, G., et al. (2017). Synthesis and properties of a lead-free hybrid double perovskite: $(CH_3NH_3)_2AgBiBr_6$. *Chem. Mater.* 29, 1089–1094. doi: 10.1021/acs.chemmater.6b03944

Xiao, Z. W., Du, K.-Z., Meng, W. W., Mitzi, D. B., and Yan, Y. F. (2017). Chemical origin of the stability difference between copper(I)- and silver(I)-based halide double perovskites. *Angew. Chem. Int. Ed.* 129, 12275–12279. doi: 10.1002/anie.201705113

Xiao, Z. W., Meng, W. W., Saparov, B., Duan, H.-S., Wang, C. L., Feng, C. B., et al. (2016). photovoltaic properties of two-dimensional $(CH_3NH_3)_2Pb(SCN)_2I_2$ perovskite: a combined experimental and density functional theory study. *J. Phys. Chem. Lett.* 7, 1213–1218. doi: 10.1021/acs.jpclett.6b00248

Yin, W.-J., Shi, T. T., and Yan, Y. F. (2014a). Unusual defect physics in $CH_3NH_3PbI_3$ perovskite solar cell absorber. *Appl. Phys. Lett.* 104:063903. doi: 10.1063/1.4864778

Yin, W.-J., Shi, T. T., and Yan, Y. F. (2014b). Unique properties of halide perovskites as possible origins of the superior solar cell performance. *Adv. Mater.* 26, 4653–4658. doi: 10.1002/adma.201306281

Zhao, X. G., Yang, D. W., Sun, Y. H., Li, T. S., Zang, L. J., Yu, L. P., et al. (2017). Cu-In Halide Perovskite (CIHP) solar absorbers. *J. Am. Chem. Soc.* 139, 6718–6725. doi: 10.1021/jacs.7b02120

Conflict of Interest: The authors declare that the research was conducted in the absence of any commercial or financial relationships that could be construed as a potential conflict of interest.